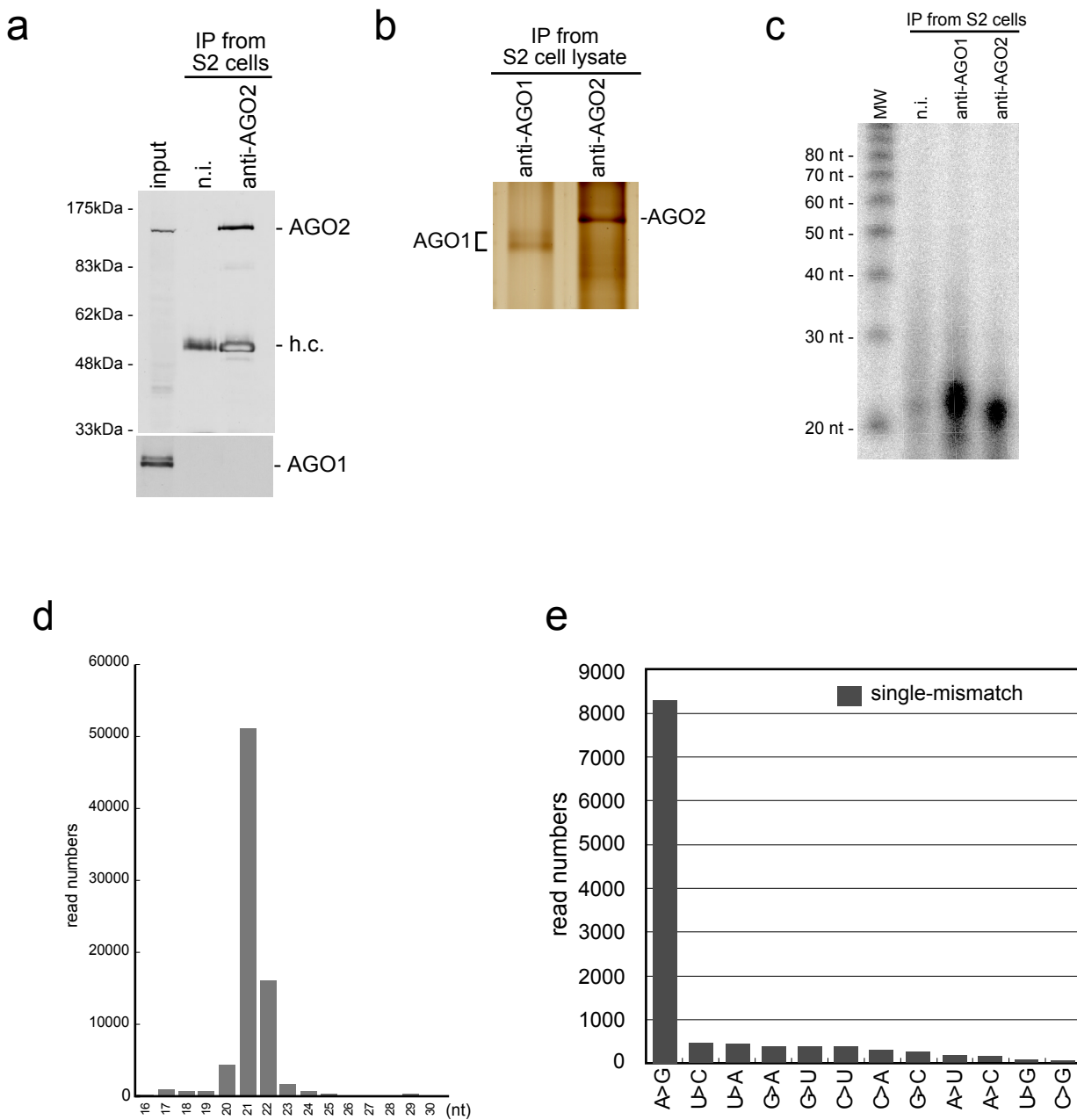


**Table of contents:**

Supplementary Figure 1-9

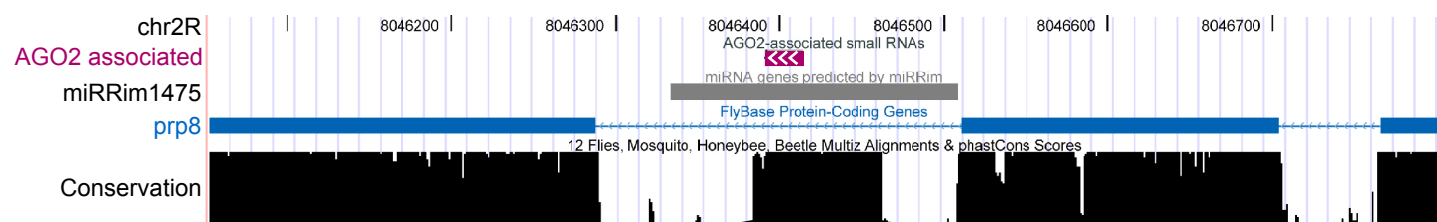
Supplementary Table 1-3

Supplementary References



**Supplementary Figure 1. AGO2 immunoprecipitation from S2 cells.** **a**, Anti-AGO2 immunoprecipitates AGO2 from S2 cells but not AGO1 protein. The immunoprecipitates with anti-AGO2 in a buffer containing Empigen were probed with anti-AGO2 and anti-AGO1. n.i.: non-immune IgG (negative control), h.c.: heavy chains of antibodies. **b**, S2 cell lysate was prepared and immunoprecipitation was performed using anti-AGO1 and anti-AGO2 from each half of the S2 cell lysate. After extensive wash, immunoprecipitates were separated on an SDS-PAGE gel and stained with silver. The amount of AGO2 immunopurified was about 3-fold higher compared with that of AGO1 protein. **c**, Small RNAs associated with AGO1 and AGO2 in S2 cells were visualized by [<sup>32</sup>P]ATP labeling. Small RNAs of ~21 nt long are detected with AGO2. miRNAs with AGO1 are about 20-22 nt long. **d**, Size distribution of AGO2-associated small RNAs. **e**, The majority of AGO2-associated small RNAs with single-mismatches show an overabundance of A-to-G (A>G), probably representing A-to-I editing.

a

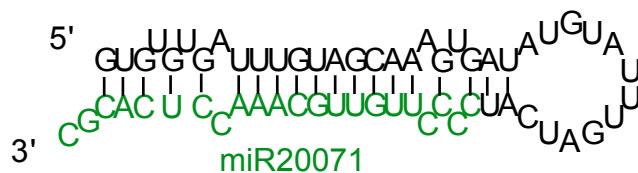


b

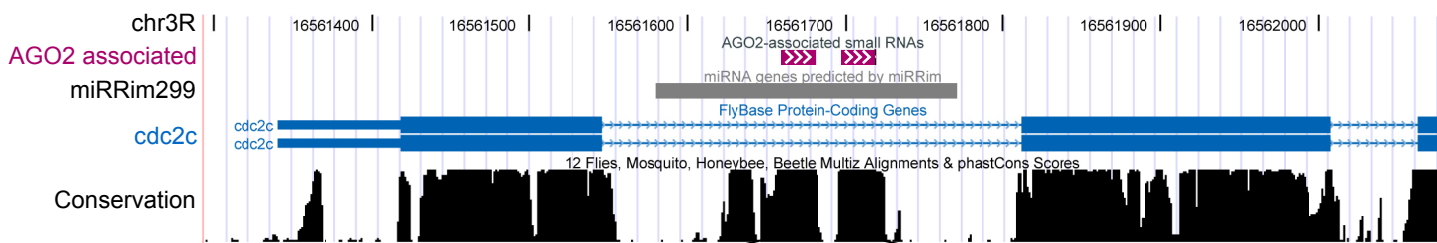
D. melanogaster	CCGGGCAUUUUGG	GUGUGUGAUUUUAGCAA	GUGUAUGUAUUUAGAUCA	CCCCUUGUUGCAAACCUACGC	CAAAGAUGAU
D. sechellia	CCGGGCAUUUUGG	GUGUGUGAUUUUAGCAA	GUGUAUGUAUUUAGAUCA	CCCCUUGUUGCAAACCUACGC	CAAAGAUGAU
D. simulans	CCGGGCAUUUUGG	GUGUGUGAUUUUAGCAA	GUGUAUGUAUUUAGAUCA	CCCCUUGUUGCAAACCUACGC	CAAAGAUGAU
D. erecta	CCGGGCAUUUUGG	GUGUGUGAUUUUAGCAA	GUGUAUGUAUUUAGAUCA	CCCCUUGUUGCAAACCUACGC	GAAGGUGAC
D. yakuba	CUGGGCAUUUUGG	GUGUGUGAUUUUAGCAA	GUGUAUGUAUUUAGAUCA	CCCCUUGUUGCAAACCUACGC	CAAAGGUGAC
D. ananassae	CUGGACAUUUUGG	GUGUGUGAUUUUAGGGCAA	GUGAUAGGUUUUAGAUCA	CCCCUUGUUGCAAACCUACGC	CCAAGGUGCU

Sequence alignment of prp8 across Drosophila species. The sequence is highly conserved, with variations highlighted in red. The alignment ends with a series of asterisks and brackets indicating structural elements.

c



d

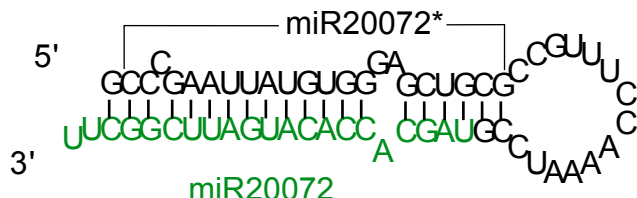


e

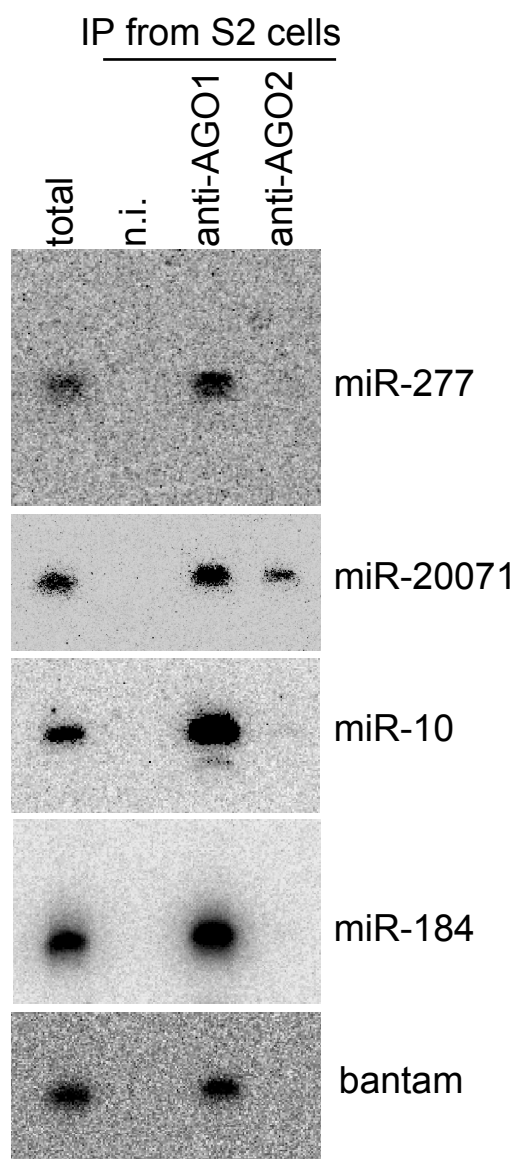
D. melanogaster	ACCUGCACCCCG	CAGCCGAAUUAUGUGGGAGCU	CGCCGUUUCCGUAAUCGUAGCACCAUAGAUUCGGCUU	CGUGGUACAGGA
D. ananassae	GCCUGGUCCUACG	CAGCCCGGAUUCUGUGGGAGCU	CGCCGUUCUUJCUAUCCGUAGCACCAUAGAUUCGGCUU	CGUGGUGCAGGG
D. erecta	ACCUGCACCCCG	CAGCCGAAUUAUGUGGGAGCU	CGCUGUUUJCUAGGAUCCGUAGCACCAUAGAUUCGGCUU	CGUGGUGCAGGA
D. yakuba	ACCUGCACCCCG	CAGCCGAAUUAUGUGGGAGCU	CGCCGUUUCLUAAGGUCCGUAGCACCAUAGAUUCGGCUU	CGUGGUGCAGGA
D. sechellia	ACCUGUACCCCG	CAGCCGAAUUAUGUGGGAGCU	CGCCGUUUCCGAAGUCCGUAGCACCAUAGAUUCGGCUU	CGUGGUGCAGGA
D. simulans	ACCUGUACCCCG	CAGCCGAAUUAUGUGGGAGCU	CGCCGUUUCCAAAGUCCGUAGCACCAUAGAUUCGGCUU	CGUGGUGCAGGA

Sequence alignment of cdc2c across Drosophila species. The sequence is highly conserved, with variations highlighted in red. The alignment ends with a series of asterisks and brackets indicating structural elements.

f



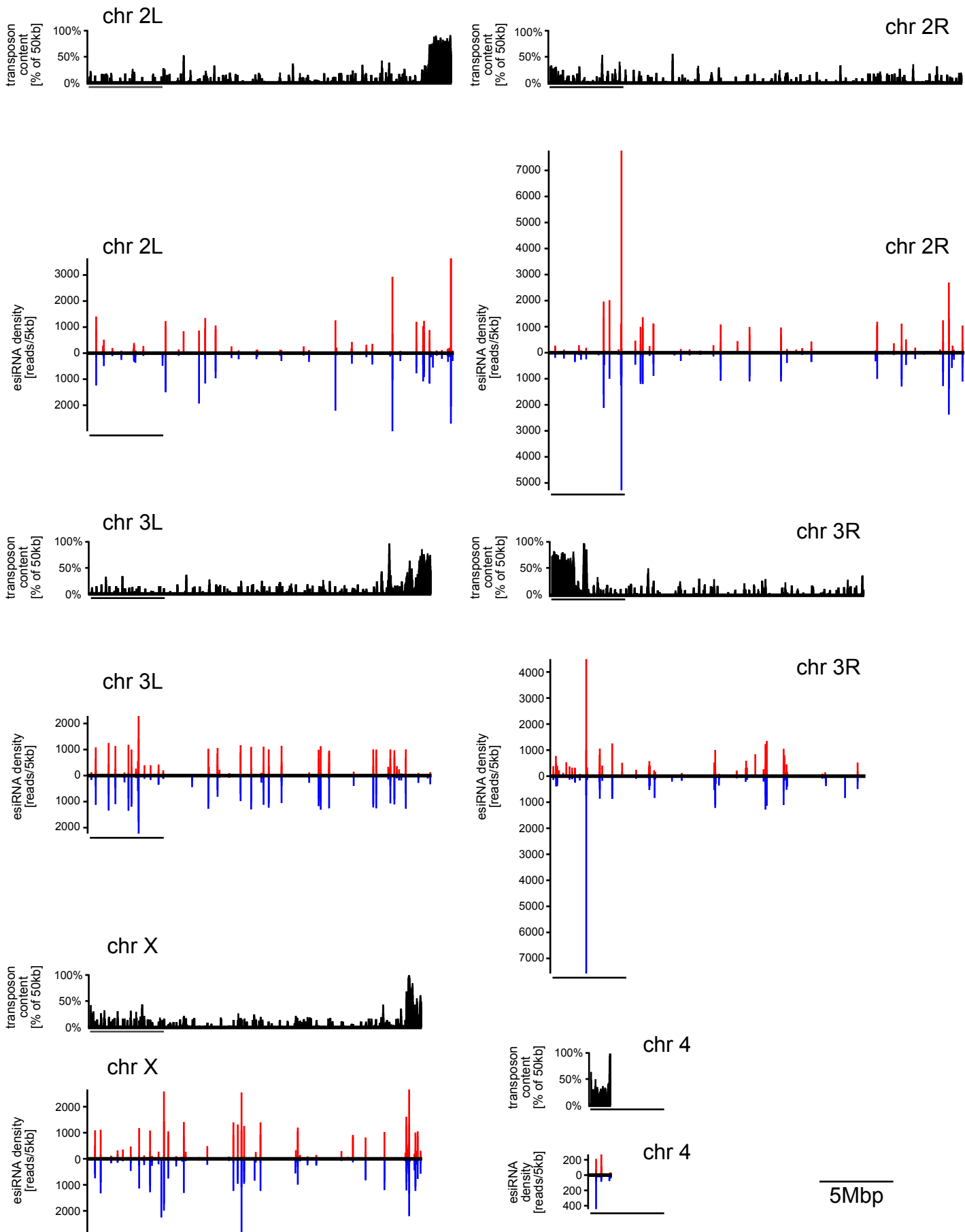
**Supplementary Figure 2. Details of two putative miRNA precursors.** **a**, A novel miRNA candidate is spotted in a highly conserved *prp8* intron (chr2R:8,046,371-8,046,482). We named this miR-20071. miRRim<sup>S1</sup>; a computational miRNA precursor finding software detects the existence of a potential miRNA gene in this region. **b**, A multiple sequence alignment of this genomic region. The region shown in red corresponds to the sequence “CCCCUUGUUGCAAACCUACAGC” (183 reads) in the reverse strand, which is also represented in the green region in a putative stem-loop structure (**c**) as a probable 3' mature miRNA of this putative miRNA. **d**, Another novel miRNA candidate is spotted in a highly conserved *cdc2* intron (chr3R:16,561,621-16,561,750). The miRRim prediction supports evidence of the potential miRNA gene. Accordingly, we named this miR-20072. “UAGCACCAACAUGAUUCGGCUU” (miR-20072; 108 reads) correspond to the red region in (**e**). **f**, The stem-loop structure of miR-20072. The mature region is shown in green. The passenger strand of miR-20072 [miR-20072\*; “CCCGAAUUAUGUGGGAGCUGCG” (2 reads)] also appeared as an AGO2-associated small RNA in this study.



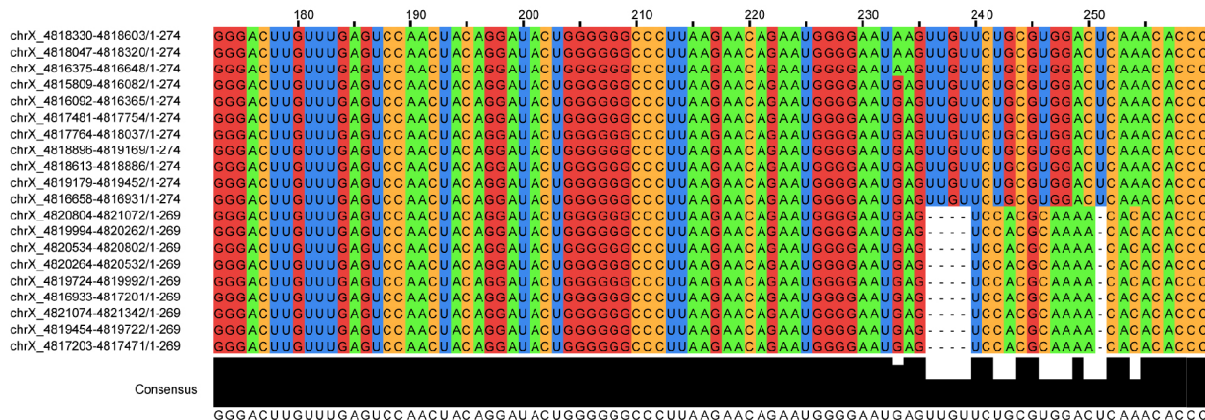
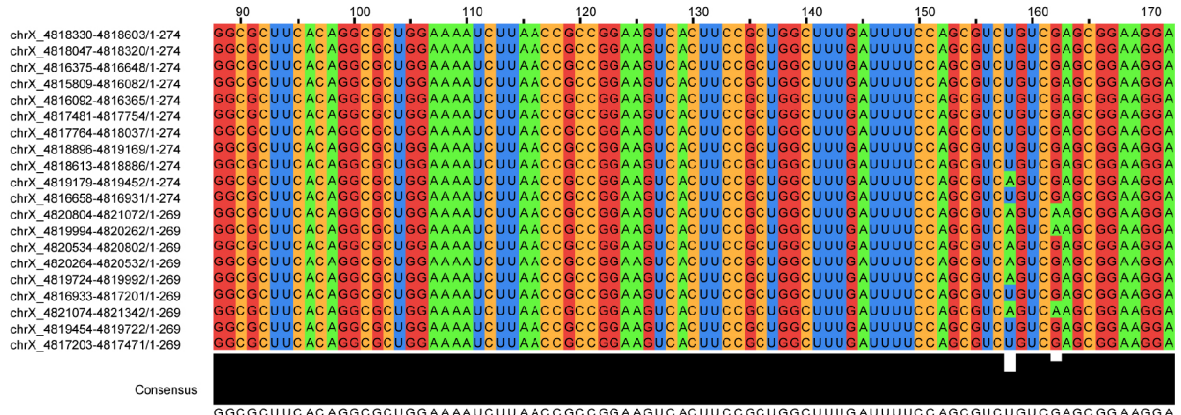
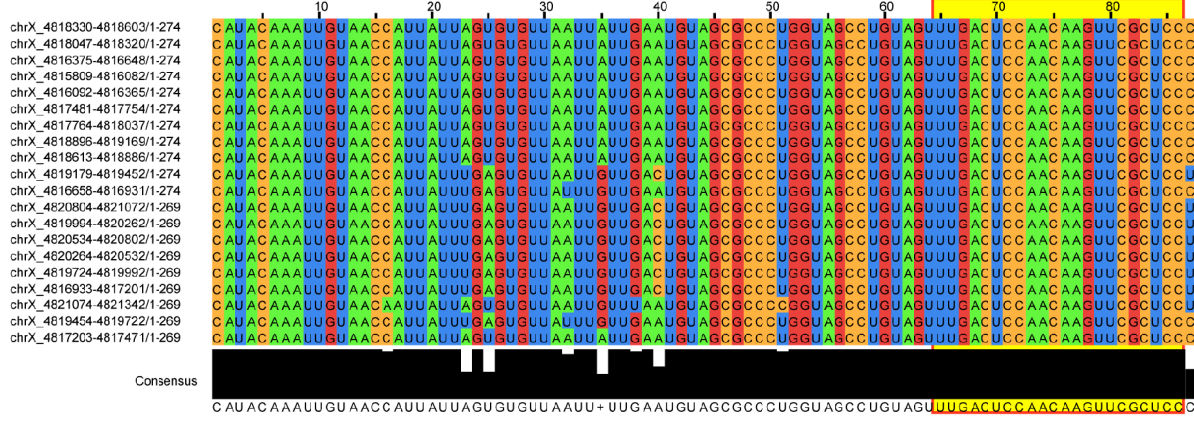
**Supplementary Figure 3. Northern blot analyses of miRNAs associated with AGO1 and AGO2.** Immunoprecipitation was performed from S2 cells using anti-AGO1 and anti-AGO2. RNAs isolated from the immunoprecipitates were probed for miR-277, miR-20071 (one of the miRNAs newly found in this study), miR-10 (miRNA appeared most often in this study; 235 in total of 64,588), miR-184 and bantam. Of these, only a minority of miR-20071 were found to be loaded onto AGO2. n.i.: non-immune IgG (negative control).

*Discussion:* Recent studies have shown that the structure of a double-stranded small RNA intermediate strongly influences its partitioning between AGO1- and AGO2-RISC (RNA-induced silencing complex)<sup>S2</sup>. Indeed, miR-277, which has a miRNA/miRNA\* duplex that resembles a siRNA duplex, was shown to be loaded onto AGO2<sup>S3</sup>. However, miR-277 did not appear at all in the sequenced small RNAs. Northern blot analysis revealed that miR-277 and others like miR-10, miRNA appeared most often in this study, and bantam were specifically observed with AGO1, supporting the belief that the vast majority of miRNAs are selectively loaded onto AGO1 at least in S2 cells<sup>S4, S5</sup>.

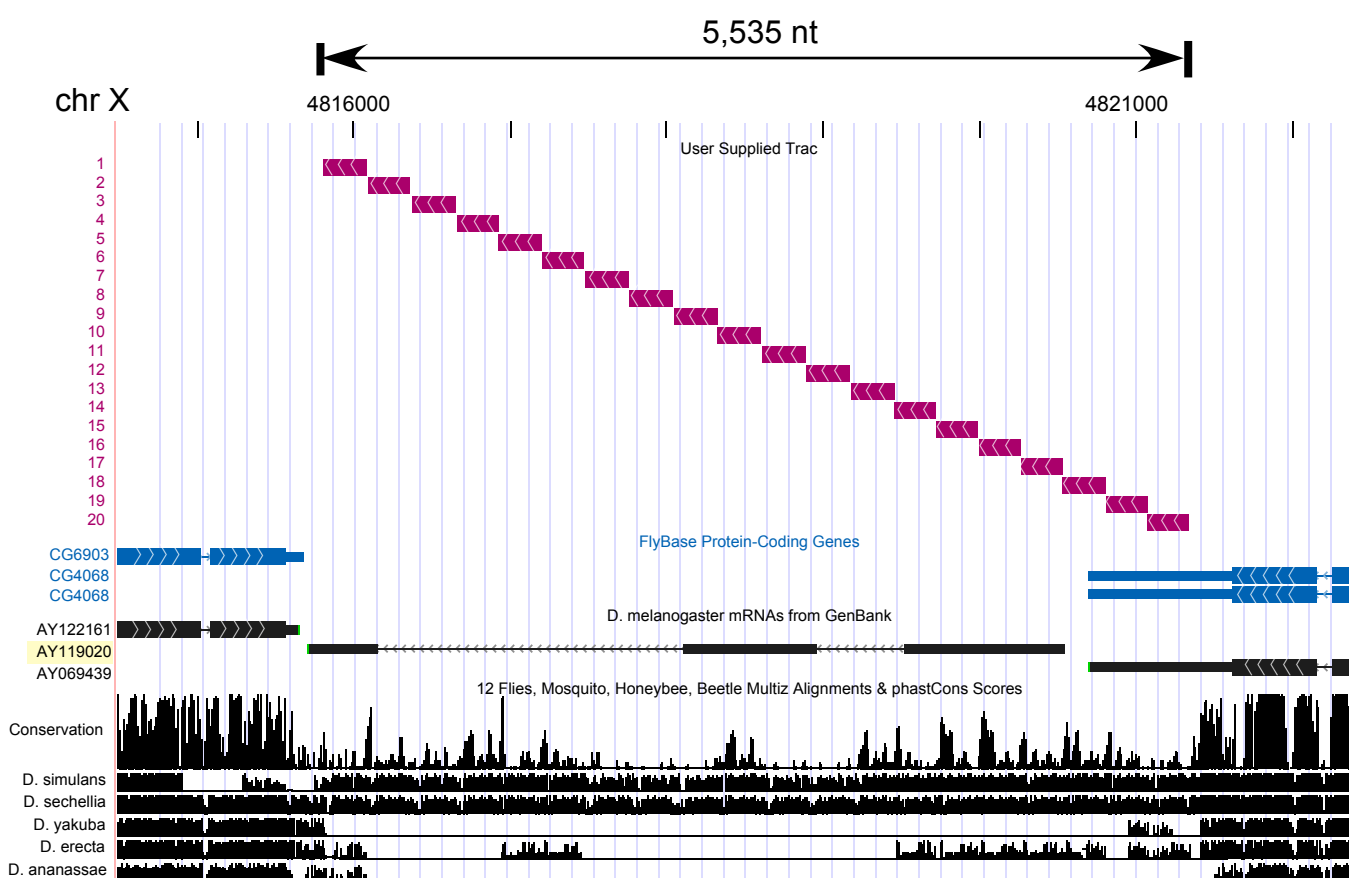
Probes used for miR-277, miR-20071, miR-184 and miR-10 are as follows;  
miR-277: 5'-TCGTACCAGATAGTGCATTT-3',  
miR-20071: 5'-GCGTGAGGTTGCAACAAGGGG-3',  
miR-184: 5'-GCCCTTATCAGTTCTCCGTCCA-3',  
miR-10: 5'-AACAAATTGGATCTACAGGGT-3'.



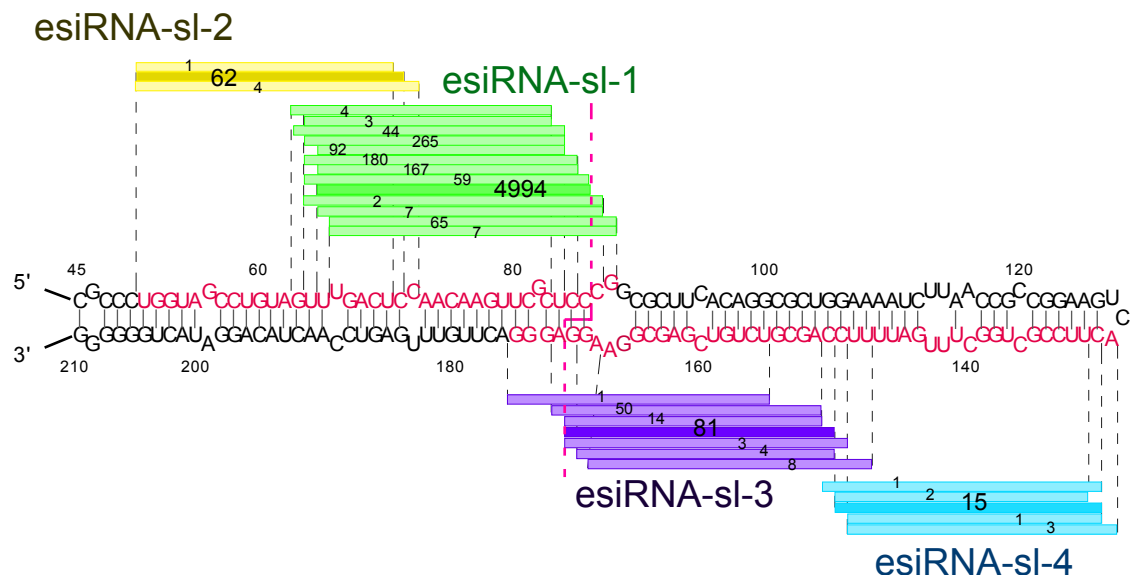
**Supplementary Figure 4. Density maps of transposons and AGO2-associated small RNAs.** The horizontal axis represents the chromosomal position. The vertical axis represents the percent content of transposons per 50kbp or the number of reads of all mapped small RNAs per 5kbp. We use flyBase natural transposons and RepeatMasker for the transposons (LINE, SINE, LTR and DNA). The density of small RNAs is rendered in red color for plus strands and blue color for minus strands. All mapping data are available from UCSC GenomeBrowser for Functional RNAs<sup>S6</sup> (<http://www.ncrna.org/>).

**a**

b



C



d

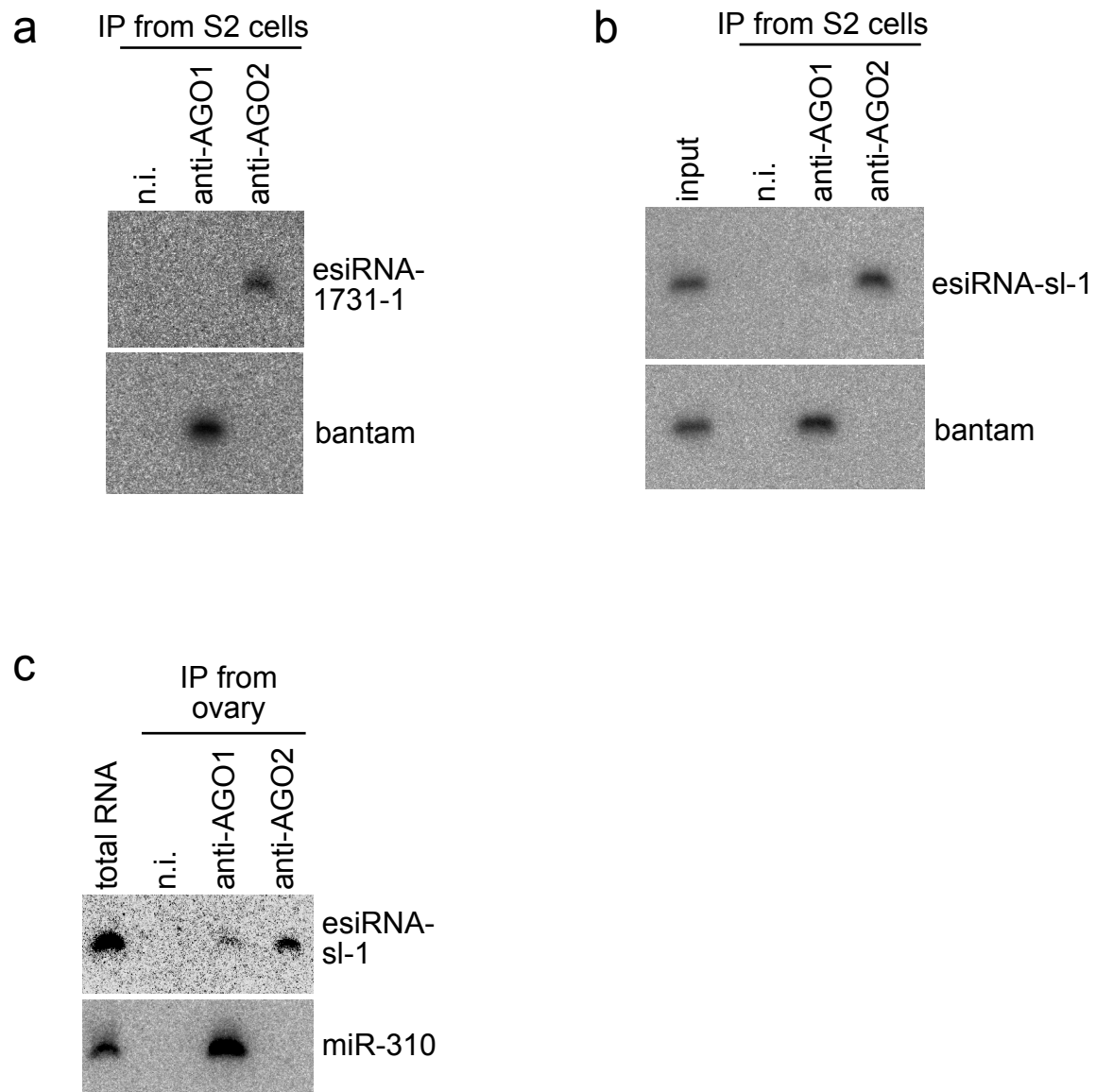
start	sequence	end	reads	sub total
51	UGGUAGCCUGUAGUUUGACU	70	1	67
51	UGGUAGCCUGUAGUUUGACUC	71	62	
51	UGGUAGCCUGUAGUUUGACUCC	72	4	
63	GUUUGACUCCAACAAGUUCGC	83	4	5889
63	GUUUGACUCCAACAAGUUCGCU	84	44	
64	-UUUGACUCCAACAAGUUCGC	83	3	
64	-UUUGACUCCAACAAGUUCGCU	84	265	
64	-UUUGACUCCAACAAGUUCGCUCC	85	180	
64	-UUUGACUCCAACAAGUUCGCUCC	86	59	
64	--UUGACUCCAACAAGUUCGCU	87	2	
65	--UUGACUCCAACAAGUUCGCU	84	92	
65	--UUGACUCCAACAAGUUCGCU	85	167	
65	--UUGACUCCAACAAGUUCGCUCC	86	4994	
65	--UUGACUCCAACAAGUUCGCUCC	87	7	
66	--UGACUCCAACAAGUUCGCUCC	86	65	
66	--UGACUCCAACAAGUUCGCUCC	87	7	
129	ACUUCCGCUGGCUUUGAUUUU	149	3	22
130	-CUUCCGCUGGCUUUGAUUUU	149	1	
130	-CUUCCGCUGGCUUUGAUUUUC	150	15	
130	-CUUCCGCUGGCUUUGAUUUUCC	151	1	
131	--UUCCGCUGGCUUUGAUUUUC	150	2	
148	UUCCAGCGUCUGUCGAGCGGA	169	8	161
150	--CCAGCGUCUGUCGAGCGGAAGG	171	3	
151	--CAGCGUCUGUCGAGCGGAAG	170	4	
151	--CAGCGUCUGUCGAGCGGAAGG	171	81	
152	----AGCGUCUGUCGAGCGGAAGG	171	14	
152	----AGCGUCUGUCGAGCGGAAGGA	172	50	
156	-----UCUGUCGAGCGGAAGGG	175	1	

Total 6139

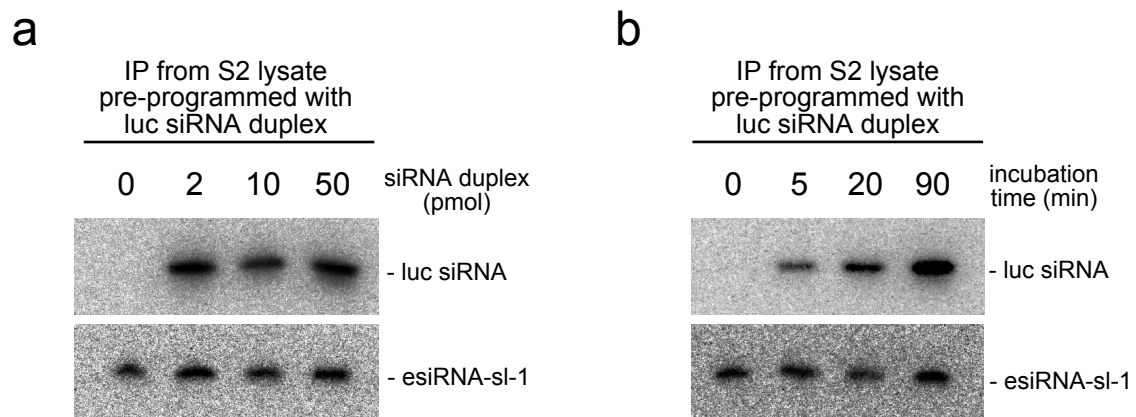
Page 3/3

**Supplementary Figure 5. esiRNA-sls are derived from an intergenic region**

**a,** A multiple sequence alignment of highly similar repetitive genomic elements (~274 nt) found in the intergenic region (chrX:4,815,808-4,821,360). The region corresponds to esiRNA-sl-1, which is mapped to the minus strand of this region; and indicated with a yellow rectangle (the first row). **b,** An overview of the intergenic region (chrX:4,815,808-4,821,360). This repetitive element is located between two coding genes, CG6903 and CG4068, on Chromosome X, spanning 5,535 nt. A unit of ~274 nt found twenty times in this region is indicated with a pink box. This region was found to be highly conserved in *D. simulans*, and *D. sechellia*, and moderately conserved in *D. erecta*. **c,** The predicted structure of a ~274 nt fragment, from which esiRNA-sl-1 originates, is shown. esiRNA-sl-1 and its siblings are indicated with green lines. The numbers indicated on the lines show the frequencies of each sequence appearing in the AGO2-associated small RNA profiling study. esiRNA-sl-2, -3, and -4, including their siblings, are indicated with yellow, purple and blue lines, respectively. Nucleotide sequences found in these esiRNAs are indicated in red on the hairpin structure. **d,** The sequences and read numbers of esiRNA-sls shown in (a) are summarized. Of each esiRNA-sl, the most frequently appearing sequence is highlighted by a darker color.

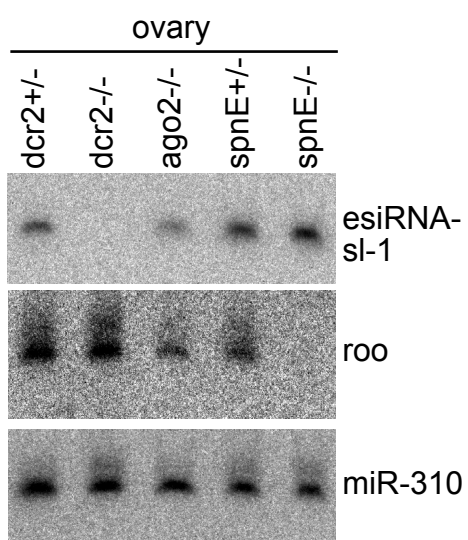


**Supplementary Figure 6. Specific association of esiRNAs with AGO2, and esiRNA-sl-1 detection in fly ovaries.** **a**, RNAs bound with AGO1 and AGO2 were probed for esiRNA-1731-1 and bantam miRNA. **b**, RNAs bound with AGO1 and AGO2 were probed for esiRNA-sl-1 and bantam. **c**, Immunoprecipitation was performed from wild-type ovary lysate using anti-AGO1 and anti-AGO2. RNAs isolated from the immunoprecipitates were probed for esiRNA-sl-1 and miR-310. As in S2 cells, esiRNA-sl-1 is specifically detected with AGO2. n.i.: non-immune IgG (negative control).



**Supplementary Figure 7. Exogenous siRNA does not displace esiRNA**

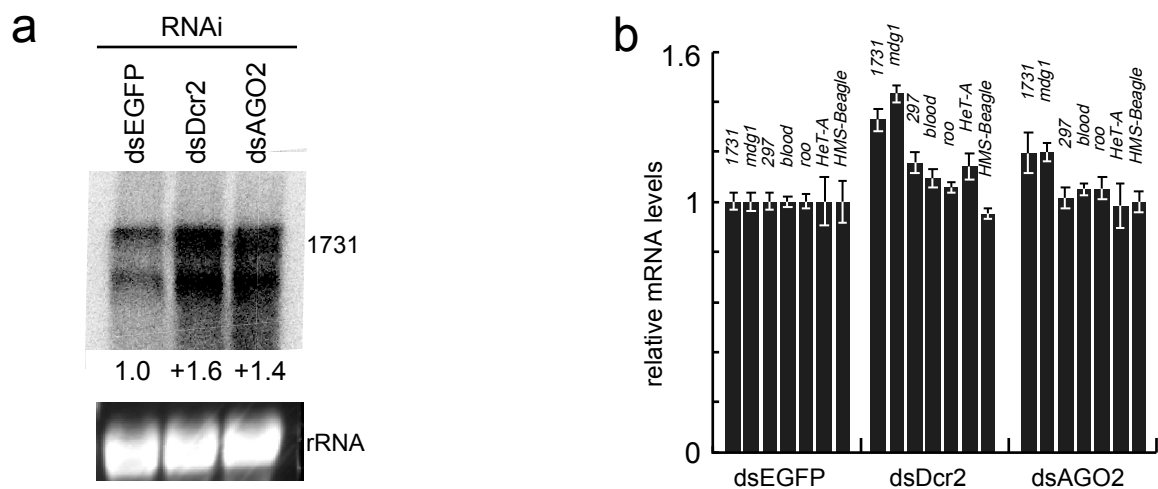
**associated with AGO2.** **a**, S2 cell lysates were prepared as described<sup>21</sup> and lucsiRNA duplex was exogenously added to the lysates<sup>21</sup>. The amounts of siRNA added to the lysates (100 µl) were 0, 2, 10, and 50 pmol as indicated. After 1h incubation at 26°C to arrow RISC formed, AGO2 was immunopurified using anti-AGO2 and RNAs associated with AGO2 were eluted. RNA pools were then divided into two and subjected to northern blotting analyses using DNA oligos recognizing luc guide siRNA and esiRNA-sl-1. It is noted that even excess amount of exogenous siRNA (50 pmol) did not displace esiRNA (esiRNA-sl-1) from AGO2. **b**, S2 cell lysate was prepared as in **(a)** and luc siRNA duplex (10 pmol) was added to the lysate. After incubation for 5, 20, and 90 min at 26°C to arrow RISC formed, AGO2 was immunopurified and RNAs associated with AGO2 were eluted. RNA pools were then analyzed by northern blotting analyses as in **(a)**. Longer incubation of time arrowed more luc guide siRNA associated with AGO2 within the lysate; however, the amount of endogenous siRNA (esiRNA-sl-1) with AGO2 did not decrease even after 90 min incubation, indicating that exogenous siRNA did not displace from AGO2.



**Supplementary Figure 8. Involvement of Dicer2 (Dcr2) in esiRNA**

**biogenesis.** Only in homozygous *dcr2* mutant ovary, is esiRNA-sl-1 undetected.

By contrast, loss of *spn-E* expression does not affect the accumulation of esiRNA-sl-1 where roo piRNA accumulation failed severely. miR-310 expression levels are unaltered in all mutant ovaries used in this experiment.



**Supplementary Figure 9. Depletion of Dicer2 or AGO2 coincided with higher levels of retrotransposon transcripts.** **a**, Dcr2 or AGO2 depletion results in the accumulation of retrotransposon transcript levels. Northern analysis of the 1731 element (left). **b**, RNA expression from retrotransposons was measured in Dcr2 or AGO2 depleted S2 cells by quantitative RT-PCR (right). Values show relative to those with EGFP dsRNA-treated cells (control).

**Table S1. The list of miRNAs in AGO2-associated small RNAs**

Sequence	read	miRNA
ACCCUGUAGAUCCGAAUUUGUU	235	
ACCCUGUAGAUCCGAAUUUGU	16	
CCCUGUAGAUCCGAAUUUGUU	3	mir-10-5p
ACCCUGUAGAUCCGAAUUUG	2	
UACCCUGUAGAUCCGAAUUUGU	2	
CAUCUUACCGGGCAGCAUUAGA	13	
CAUCUUACCGGGCAGCAUUAG	3	
AUCUUACCGGGCAGCAUUAGA	2	mir-8-5p
CAUCUUACCGGGCAGCAUUA	1	
CAUCACAGUCUGAGUUCUUGC	2	
CAUCACAGUCUGAGUUCUUGC	1	mir-11-3p
UAUCACAGCCAUUUUGACGAGU	1	mir-13b-1-3p,mir-13b-2-3p
GUGCAUUGUAGUCGCAUUGUC	41	
GUGCAUUGUAGUCGCAUUGU	10	mir-33-5p
UAAAGCUAGAUUACCAAAGCAU	26	mir-79-3p
CAUUGCACUUGUCCCGGCCUAU	36	
CAUUGCACUUGUCCCGGCCUA	3	mir-92a-3p
AAAUGCACUAGUCCCGGCCUG	9	
AAAUGCACUAGUCCCGGCCU	3	
AAUUGCACUAGUCCCGGCCUG	2	mir-92b-3p
AAUUGCACUAGUCCCGGCCUGC	1	
CCUUAUCAUUCUCUCGCCCCG	12	
CCUUAUCAUUCUCUCGCCCCGU	11	mir-184-5p
UGGACGGAGAACUGUAAGGGC	6	
GGACGGAGAACUGUAAGGGC	1	mir-184-3p
UAGGAACUUCAUACCGUGCUCU	1	mir-276a-3p
UGACUAGAUCCACACUCAAUA	99	
UGACUAGAUCCACACUCAAUA	16	
UGACUAGAUCCACACUCAU	6	mir-279-3p
UGACUAGAUCCACACUCAU	2	
AAUCACAGGAUUAACUGUGA	4	
CACAGGAUUAACUGUGAG	2	
CAGGAUUAACUGUGAG	2	
AAAUCACAGGAUUAACUGUGA	2	mir-308-3p
AUCACAGGAUUAACUGUGAG	1	
AAUCACAGGAUUAACUGUGAG	1	
AUCACAGGAUUAACUGUGA	1	
CCCCUUGUUGCAAACCUCACGC	183	
CCCCUUGUUGCAAACCUCACG	23	
CCCCUUGUUGCAAACCUCACGCC	2	mir-20071
CCCUUGUUGCAAACCUCACGCC	1	
CCCUUGUUGCAAACCUCACGC	1	
CCCGAAUUAUGUGGGAGCUGCG	2	mir-20072-5p
UAGCACCCACAUGAUUCGGCU	108	
UAGCACCCACAUGAUUCGGCU	11	mir-20072-3p
UAGCACCCACAUGAUUCGG	2	

**Table S2. Cluster analysis of AGO2-associated small RNAs.**

chrom	start	end	length (bp)	all RNAs in this cluster	cluster unique RNAs	strand distribution (+/- in %)
chr2R	8,046,391	8,046,414	24	210	210	0/100
chr3R	16,561,660	16,561,719	60	123	123	100/0
chrU	3,998,711	4,029,320	30,610	151	102	41.2/58.79
chrU	5,741,256	5,830,216	88,961	115	63	78.86/21.13
chr3RHet	618,188	891,223	273,036	294	43	55.53/44.46
chr2R	6,438,850	6,444,437	5,588	43	43	36.99/63
chrU	1,132,229	1,153,494	21,266	697	42	58.22/41.77
chrU	7,475,614	7,550,072	74,459	270	35	39/60.99
chr3L	8,663,848	8,686,778	22,931	35	35	42.85/57.14
chr2R	2,145,493	2,239,087	93,595	1,119	32	34.69/65.3
chr3R	4,720,667	4,732,086	11,420	908	22	57.93/42.06
chr3LHet	238,159	685,011	446,853	113	21	54.44/45.55
chr2L	21,081,541	21,108,660	27,120	21	21	57.14/42.85
chr3L	11,322,867	11,325,912	3,046	35	20	75.15/24.84
chr2L	117,255	195,336	78,082	20	20	75/25
chr2L	470,102	502,949	32,848	17	17	35.29/64.7
chr2L	12,519,661	12,528,195	8,535	17	17	0/100
chrU	8,748,038	9,349,808	601,771	899	14	40.86/59.13
chr3L	3,231,478	3,251,102	19,625	14	14	92.85/7.14
chr2L	858,871	863,926	5,056	14	14	78.57/21.42
chr3LHet	723,452	814,976	91,525	302	13	50.24/49.75
chr3R	26,597,879	26,600,759	2,881	12	12	91.66/8.33
chr3LHet	842,861	905,466	62,606	805	11	56.58/43.41
chrU	4,545,313	4,585,483	40,171	276	10	55.27/44.72
chr3R	2,903,684	2,927,095	23,412	10	10	100/0
chrX	2,071,839	2,076,040	4,202	10	10	0/100
chr3L	19,066,801	19,087,947	21,147	10	10	80/20
chr3L	4,244,470	4,260,408	15,939	9	9	55.55/44.44
chr3R	8,807,662	8,854,508	46,847	9	9	55.55/44.44
chr3L	22,799,752	22,822,404	22,653	9	9	1.23/98.76
chr3L	3,096,596	3,096,962	367	9	8	26.59/73.4
chr3R	22,694,426	22,697,615	3,190	8	8	25/75
chr3R	9,289,996	9,290,018	23	8	8	0/100
chr3R	17,434,854	17,447,644	12,791	8	8	3.66/96.33
chrX	21,394,207	21,426,731	32,525	176	7	56.72/43.27
chr2L	7,970,313	8,023,444	53,132	82	7	55.23/44.76
chr2R	1,610,257	1,649,680	39,424	8	7	58.86/41.13

chr3L	20,515,307	20,515,415	109	7	7	0/100
chr2R	6,403,263	6,417,380	14,118	7	7	71.42/28.57
chrX	1,758,627	1,772,418	13,792	7	7	28.57/71.42
chr2R	2,509,795	2,546,428	36,634	7	7	14.49/85.5
chr3R	17,097,297	17,097,320	24	7	7	100/0
chr2L	1,145,826	1,153,500	7,675	7	7	14.28/85.71
chr3R	9,607,594	9,607,615	22	7	7	0/100
chr2L	420,299	420,395	97	7	7	0/100
chr3L	9,420,556	9,432,105	11,550	7	7	28.57/71.42
chr2L	21,691,974	21,761,803	69,830	13	6	69.75/30.24
chr3L	19,791,124	19,792,543	1,420	6	6	83.33/16.66
chr3R	7,478,952	7,480,399	1,448	6	6	0/100
chr3L	3,379,359	3,379,660	302	6	6	0/100
chr3R	4,630,503	4,655,467	24,965	6	6	83.33/16.66
chr2R	8,460,021	8,477,775	17,755	6	6	66.66/33.33
chr2LHet	123,291	219,338	96,048	251	5	43.73/56.26
chr2RHet	309,994	524,143	214,150	144	5	52.61/47.38
chrX	13,892,300	13,901,124	8,825	51	5	0.92/99.07
chr3R	21,150,271	21,154,896	4,626	6	5	72.42/27.57
chrX	1,962,402	1,974,073	11,672	5	5	60/40
chr2R	17,018,597	17,032,479	13,883	5	5	60/40
chr2L	6,083,979	6,084,273	295	5	5	40/60
chr2L	72,866	72,887	22	5	5	0/100
chrX	1,359,418	1,376,729	17,312	5	5	80/20

The analysis which is similar one done in Brennecke et al.<sup>9</sup>, is performed as follows: First, AGO2-associated small RNAs are mapped onto the *D. melanogaster* genome. Hits with any mismatch are discarded. Also we discard hits overlap with known miRNAs, rRNAs, tRNAs, other ncRNAs (flyBase noncoding genes) and sense strands of known coding genes (flyBase genes). We assign a weight score for each hit where the weight is defined as a ratio of cloning frequency over number of mappings of each sequence. Groups of neighboring hits within 1kb form a cluster. Clusters located less than 20kb each other are merged as one cluster. Valid clusters should contain more than five uniquely mapped small RNA hits. The table is sorted in a descending order of the cluster unique RNAs. The number shown in the column “all RNAs in this cluster” is the sum of the weight scores for all RNAs included in each cluster. The number shown in the column “cluster unique RNAs” is the sum of the weight scores for all uniquely mapped RNAs included in each cluster.

**Table S3. Primers for quantitative PCR**

Detects	sequence (forward primer, reverse primer)
<i>RP49</i>	CCGCTTCAAGGGACAGTATCTG, ATCTGCCGCAGTAAACGC
<i>1731</i>	TATGGGCTGAGGCATAAAC, CAAGTGGCTCACTGCTGGTA
<i>mdg1</i>	AACAGAAACGCCAGCAACAGC, CGTCCCAGTCCGTTGTGAT
<i>297</i>	CTGGCAAAGGGATTTCATCA, TGCATTCTAAGGCCAAATG
<i>blood</i>	TATCGCATGGCAGATAGCCAAA, CGTGGATTAGCGGAAGTGTTTC
<i>roo</i>	CGTCTGCAATGTACTGGCTCT, CGGCACCTCCACTAACTTCTCC
<i>HeT-A</i>	CGCGCGGAACCCATCTTCAGA, CGCCGCAGTCGTTGGTGAGT
<i>HMS-Beagle</i>	CAAACCATGCGGCGAATAA, TTGACGGCTGAAAATTGC

### **Supplementary References:**

- S1. Terai, G., Komori, T., Asai, K. & Kin, T. miRRim: A novel system to find conserved miRNAs with high sensitivity and specificity. *RNA* **13**, 2081-2090 (2007).
- S2. Tomari, Y., Du, T. & Zamore, P. D. Sorting of Drosophila small silencing RNAs. *Cell* **130**, 299-308 (2007).
- S3. Förstemann, K., Horwich, M. D., Wee, L., Tomari, Y. & Zamore P. D. *Drosophila* microRNAs are sorted into functionally distinct argonaute complexes after production by dicer-1. *Cell* **130**, 287-297 (2007).
- S4. Okamura, K., Ishizuka, A., Siomi, H. & Siomi, M.C. Distinct roles for Argonaute proteins in small RNA-directed RNA cleavage pathways. *Genes Dev.* **18**, 1655-1666 (2004).
- S5. Miyoshi, K., Tsukumo, H., Nagami, T., Siomi, H. & Siomi, M. C. Slicer function of *Drosophila* Argonautes and its involvement in RISC formation. *Genes Dev.* **19**, 2837-2848 (2005).
- S6. Kin, T. *et al.* fRNAdb: a platform for mining/annotating functional RNA candidates from non-coding RNA sequences. *Nucleic Acids Res.* **35**(Database)

issue):D145-148 (2007).